

Analysis of Biologically Inspired Swarm Communication Models

Musad Haque, Electa Baker, Christopher Ren, Douglas Kirkpatrick
and Julie A. Adams

Abstract The biological swarm literature presents communication models that attempt to capture the nature of interactions among the swarm's individuals. The reported research derived algorithms based on the metric, topological, and visual biological swarm communication models. The evaluated hypothesis is that the choice of a biologically inspired communication model can affect the swarm's performance for a given task. The communication models were evaluated in the context of two swarm robotics tasks: search for a goal and avoid an adversary. The general findings demonstrate that the swarm agents had the best overall performance when using the visual model for the search for a goal task and performed the best for the avoid an adversary task when using the topological model. Further analysis of the performance metrics by the various experimental parameters provided insights into specific situations in which the models will be the most or least beneficial. The importance of the reported research is that the task performance of a swarm can be amplified through the deliberate selection of a communications model.

Keywords Artificial swarms · Robotics tasks

M. Haque (✉) · E. Baker · C. Ren · D. Kirkpatrick · J.A. Adams
Department of Electrical Engineering and Computer Science, Vanderbilt
University, Nashville, TN, USA
e-mail: musad.a.haque@vanderbilt.edu

E. Baker
e-mail: electa.a.baker@vanderbilt.edu

C. Ren
e-mail: christopher.ren@vanderbilt.edu

D. Kirkpatrick
e-mail: kirkpa48@msu.edu

J.A. Adams
e-mail: julie.a.adams@oregonstate.edu

1 Introduction

Animals that live in groups gain reproductive advantages, benefit from reduced predation risks, and forage efficiently through group hunting and the distribution of information amongst group members [20]. The collective behavior of these biological systems, for instance, trail-forming ants, schooling fish, and flocking birds, display tight coordination that appears to emerge from local interactions, rather than through access to global information or a central controller [8]. Numerical simulations based solely on local interaction rules can recreate coordinated movements of biological systems living in groups [2, 12, 17, 19, 27, 32].

Proposed communication models for group behavior in animals include the metric [11], the topological [1, 3], and the visual models [31]. The metric model is directly based on spatial proximity: two individuals interact if they are within a certain distance of one another [11]. Ballerini et al.'s [3] topological model requires each individual to interact with a finite number of nearest group members. The visual model, which is based on the sensory capabilities of animals, permits an individual to interact with other agents in its visual field [31]. The communication model is an important element in collective behavior, because it reveals how information is transferred in the group [31].

The development of communication networks is described as “one of the main challenges” in swarm robotics [18]. Bio-inspired artificial swarms inherit desirable properties from their counterparts in nature, such as decentralized control laws, scalability, and robustness [6]. Robustness in the context of this paper implies that the failure of one agent does not lead to the failure of the entire swarm. Despite the beneficial properties, a poorly designed communication network to an artificial swarm can lead to undesirable consequences, such as the swarm fragmenting into multiple components [18].

The evaluated hypothesis is that the three communication models—metric, topological, or visual—when used by a tasked artificial swarm will affect the swarm’s performance. The evaluation analyzes how the communication models impact swarm performance for two swarm robotics tasks: searching for a goal and avoiding an adversary. The findings demonstrate that there is a significant impact of the communication model on task performance, which implies that the task performance of a deployed artificial swarm is amplified through performance-based selection of communication models.

Section 2 provides related work. Section 3 describes the coordination algorithms derived from the biological models. Experiments are presented in Sects. 4 and 5. Practical applications are discussed in Sect. 6, and an overall discussion with concluding remarks is provided in Sect. 7.

2 Related Work

Comparative evaluations of swarm communication models can be grouped into three fields: biology [3, 31], physics [4, 29], and computer science [16].

Prior research compared the communication models to identify which model best explains the propagation of information within biological species. Stranburg-Peshkin et al. [31] reported that for golden shiners, *Notemigonus crysoleucas*, the visual model best predicts information transfer within the school. The Metric and topological models were compared for flocks of European starlings, *Sturnus vulgaris* [3], and the topological model most accurately described the starlings' information network. The experiment compared the cohesion of simulated swarms using the topological and metric models, and the topological model generated more cohesive swarms [3].

Physics-based approaches compared the metric and topological models and presented the resulting system properties. Specifically, Shang and Bouffanais [29] presented results on the probability of reaching a consensus. Barberis and Albano [4] analyzed the difference in group orders (alignment and moment) that arise when using the metric and topological models.

Computer science results include evaluating the metric and topological models in the context of human-swarm interaction [16]. The human steered the swarm by manipulating a leader agent that directly influenced other swarm members. It was determined that a human can more easily manage a swarm using the topological model.

The presented evaluation appears to be the first to compare the metric, topological, and visual models for tasks on artificial agents.

3 Coordination Algorithms

The agents are modeled as $2D$ self-propelled particles. A self-propelled particle is controlled through updates to its velocity heading, which in turn affects the particle's position [12, 15, 32].

The artificial agents are indexed 1 through N , where N is the number of agents in the swarm. If there is a communication link from agent $i \in \{1, \dots, N\}$ to agent $j \in \{1, \dots, N\}$, where $i \neq j$, agent j is a neighbor of agent i . The neighbor set of agent i , denoted by $\mathcal{N}_i(t)$ is the collection of all the neighbors of agent i at time t .

The coordination of the swarm agents is designed through a multi-level coordination algorithm. At the higher level of abstraction, an agent's neighbors are determined by the communication model. Thus, for agent i , the communication model constructs the set $\mathcal{N}_i(t)$ at each time t . At the lower abstraction level, agents only interact with their neighbors and the nature of this interaction is governed by three rules: repulsion, orientation, and attraction. The rules are based on Reynolds's rules for boids (see [27]), which are similar to the biological swarm literature (e.g., [2]).

Each agent's zones of repulsion, orientation, and attraction are centered at the agent's position and are parameterized through the radii r_{rep} , r_{ori} , and r_{att} , respectively, where $r_{rep} < r_{ori} < r_{att}$. The zones are represented as circles in the 2D case.

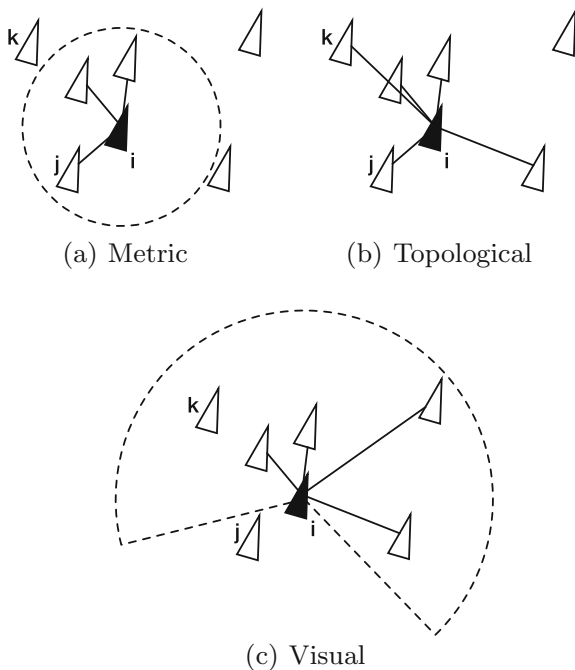
The heading of each agent $i \in \{1, \dots, N\}$ is updated as follows: (1) Veer away from all agents in $\mathcal{N}_i^r(t)$ within a distance r_{rep} , (2) Align velocity with all agents in $\mathcal{N}_i^o(t)$ that are between a distance of r_{rep} and r_{ori} , and (3) Remain close to all agents $j \in \mathcal{N}_i^a(t)$ that are between a distance of r_{ori} and r_{att} [21, 27].

3.1 Communication Models

The metric model uses a single parameter d_{met} that represents a distance measure. All agents within a distance d_{met} from agent i are i 's neighbors, as shown in Fig. 1a. Due to the symmetric nature of the model, if $j \in \mathcal{N}_i^r(t)$, then $i \in \mathcal{N}_j^r(t)$. A stochastic version of this model was developed to analyze starling data [5]. The analyzed models assign neighbors in a deterministic manner.

The topological model is characterized by n_{top} , measured in units of agents. $\mathcal{N}_i^t(t)$ is the set containing the n_{top} nearest agents from agent $i \in \{1, \dots, N\}$. Zebrafish, *Danio rerio*, have 3–5 topological neighbors [1], and starlings coordinate, on average, with the nearest 6–7 birds [3]. Figure 1b depicts the neighbors of agent i , with n_{top} set to 5.

Fig. 1 Agents (triangles) are shown in relation to the focus agent (filled triangle), labeled i . The communication links from agent i to its neighbors are represented with lines.
a Metric: Agent k is at a distance greater than d_{met} (dashed circle) from agent i ;
b Topological: n_{top} is set to 5;
c Visual: The visual range of agent i is shown (dashed sector), where agent j is in agent i 's blindspot and agent k is occluded from agent i by another agent



A sensing range, a blindspot, and occlusion are used to describe the visual model [31]. Agent j is a neighbor of agent i , if three conditions are met: (1) The distance between the two agents is less than d_{vis} , (2) Agent j is not in agent i 's blindspot, and (3) The line-of-sight between the agents is not occluded by another agent or object in the environment. A blindspot emerges because the agent's sensing range is characterized by an angle $\pm\phi$ from its heading [12, 15]. Figure 1c depicts agent i 's sensing range, with ϕ set to $2\pi/3$ radians.

The particular choices made for the values of d_{met} , n_{top} , d_{vis} , and ϕ can be characterized as inheriting from the "descriptive agenda" of multi-agent learning [22, 30]. The goal in the descriptive agenda is to model the underlying phenomenon from the social sciences (biological swarm communication models). The biological swarm literature provides parameter values that are used to compare the different communication models on tasked artificial swarms. d_{met} was set to r_{att} for metric model experiments (e.g., [2, 11]). The visual model experiments set an agent's d_{vis} to half the size of the diagonal of the world with $\phi = 2\pi/3$ radians [12, 31]. $n_{top} \in \{5, 6, 7, 8\}$ for the topological experiments, allowing some variability, while remaining close to what was observed in nature [3].

The novelty is the comparative evaluations of the different communication models that are *solely* based on the biological swarm literature; hence, strictly inheriting from a descriptive agenda. Traditional artificial swarm communication models do not typically mimic the three communication models (e.g., [9]). Although, perception-based models that rely on line-of-sight communication, such as a swarm of foot-bots responding to light sensors, is a variant of the visual model [14]. As such, one potential application is to serve as a guide for hardware selection.

4 The Search for a Goal Experiment

4.1 Experimental Design

All experiments were conducted using the Processing open-source programming language on a 8 GB, 2.6 GHz Intel Core i5 Macbook Pro. The body length, BL , of each agent was set to 2 pixels. The size of the world was 600×600 pixels.

The communication model is the primary independent variable: metric, topological, and visual. Additional independent variables were: the number of agents, the number of obstacles, the radius of repulsion, the radius of orientation, and the radius of attraction. The experiment combined each of the primary independent variables with each of the additional independent variables. The resulting pair-wise combinations offers a more comprehensive analysis of the effect of the communication models.

The number of *agents*, N , was 50, 100, and 200. The tuple $(r_{rep}, r_{ori}, r_{att})$ describes an agent's repulsion, orientation, and attraction zones. The radius of repulsion, r_{rep} , was set to either $5 \times BL$ or $10 \times BL$. The radius of orientation, r_{ori} , was assigned to

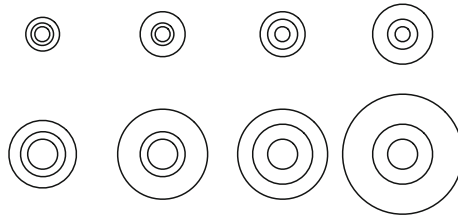
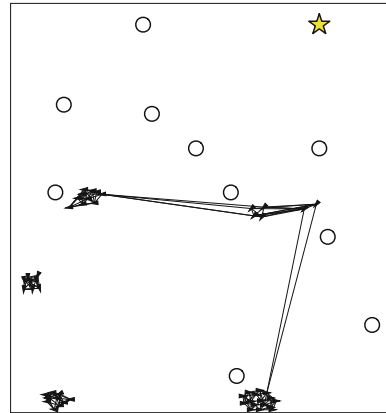


Fig. 2 The eight possible interaction zone configurations. The inner-most, middle, and outer-most circles represent the zones of repulsion, orientation, and attraction, respectively

Fig. 3 An artificial swarm performing the search for a goal task using the topological model. The center of the goal area is represented by a star, circles represent obstacles, agents are filled triangles, and the lines denote communication links. The trial parameters were: $N = 50$, $N_{obs} = 0.20N$, $r_{rep} = 20$, $r_{ori} = 40$, $r_{att} = 60$, and $n_{top} = 6$



either $1.50 \times r_{rep}$ or $2.00 \times r_{rep}$, and the radius of attraction, r_{att} , was given a value of either $1.50 \times r_{ori}$ or $2.00 \times r_{ori}$. Designing the interaction zones in this manner results in 2^3 possible tuples with varying (relative) zone sizes, as illustrated in Fig. 2.

The search for a goal task included *environmental* obstacles. The number of obstacles, N_{obs} , was 0%, 10%, or 20% of N .

The objective of the artificial swarm during the *search for a goal* is to locate a single goal location,¹ the star in Fig. 3. The goal area's size is scaled to ensure the swarm is able to fit within the goal area. The world is bounded by a wall that exerts a repulsive force. An agent can sense the goal if it is within r_{att} of the goal area's location. Once an agent locates the goal, it can communicate the location to its neighbors. Agents aware of the goal's location update their headings by equally weighing the desire to travel to the goal and the desire to follow the interaction rules, which was employed by Couzin et al. [11] and Goodrich et al. [16]. The simulation runs for 1,000 iterations.

The *percent reached*, denoted by R , determines the number of agents that reached the goal area, expressed as a percentage of the swarm's size, N , at the end of the task.

¹ Videos of example trials can be found at <http://www.eecs.vanderbilt.edu/research/hmtl/wp/index.php/research-projects/human-swarm-interaction/emulating-swarm-communications/>.

The *latency*, L , measures the rate of information transfer in the swarm during the task. Specifically, latency represents the number of iterations required for the swarm to transition from a state where at least one agent knows the goal's location to all agents being aware of the goal's location. Degenerate cases are processed by setting the latency to the maximum possible duration, 1,000 iterations. Based on this definition, the simulator did not influence this metric.

The clustering coefficient is the fraction of pairs of a swarm agent's neighbors that are neighbors with each other [13]. The coefficient ranges from 0, where none of the swarm agent's neighbors are neighbors with each other, to 1, where all pairs of a swarm agent's neighbors are neighbors with each other. The *swarm clustering coefficient*, denoted by SCC , averages the clustering coefficients of all swarm agents. A high swarm clustering coefficient implies a dense communication network and redundant information passing between the agents. While calculating the swarm clustering coefficient, the asymmetric nature of the communication links that resulted from the topological and visual models were ignored. Strandburg-Peshkin et al. [31] performed the same treatment on directed links when comparing this metric across different communication models for fish data. This metric permits comparison to prior findings.

The three hypotheses for this task are:

1. $H_{sg1}: R_V > R_T > R_M$,
2. $H_{sg2}: L_V < L_T < L_M$, and,
3. $H_{sg3}: SCC_V < SCC_T < SCC_M$.

The subscripts associated with the performance metrics indicate the metric (M), the topological (T) and the visual (V) models.

Hypothesis H_{sg1} assumes that a greater percentage of agents will reach a goal using the visual model and that the metric model will have the lowest percentage reached. The hypothesis is based on the *potentially* long-range sensing capabilities associated with the visual model. Agents favorably oriented and not occluded by obstacles or other agents have a higher chance of communicating with an agent that has located the goal. Moreover, fewer stragglers may arise with the visual and topological models, thus increasing the percent reached. H_{sg1} further assumes that the limit on n_{top} , compared to the range of d_{vis} , allows a greater percentage of agents to arrive at a goal using the visual model, compared to the topological model.

Establishing long-range communication between two agents in the visual model depends on the orientation of the agents and occluding factors. The range d_{vis} may not be a limiting factor in identifying neighbors when positioned in the interior of the swarm. However, any occurrence, regardless of how infrequent, of a long-range link in the network can act as a short-cut for transferring information. As such, H_{sg2} states that information diffuses faster in swarms using the visual and topological models, than with the metric model.

Hypothesis H_{sg3} states that the swarm clustering coefficient will be the highest in the metric model and the lowest in the visual model. Communication links in the metric and topological models are not affected by occlusions, a factor that is expected to yield sparser networks for the visual model.

A trial is defined as a single simulation run for a given selection of parameters, $(N, N_{obs}, r_{rep}, r_{ori}, r_{att})$. Twenty-five trials for each parameter selection were completed. The total number of trials for the search for a goal task was 10,800: 1,800 trials for each of the metric and visual models, and 7,200 trials for the topological model (1,800 trials for each of the four values of n_{top}).

4.2 Results

The Anderson-Darling test for normality indicated that all performance metrics: percent reached ($A = 431.01, p < 0.001$), latency ($A = 621.88, p < 0.001$), and swarm clustering coefficient ($A = 162.72, p < 0.001$) were distributed normally. An analysis of variance (ANOVA) by n_{top} did not find a significant difference for the topological model's performance. Without loss of generality, the topological trials with $n_{top} = 7$ are used in the reported ANOVAs.

The topological and visual models had virtually identical mean **percent reached**, as reported in Table 1. The ANOVA found that model type had a significant impact on the percent reached ($F(2, 5398) = 83.91, p < 0.001$). A Fisher's LSD test investigated the pair-wise differences. There was no significant difference between the visual and topological models, and the metric model had a significantly lower percent reached compared to the other models.

All data was further analyzed by the number of agents, number of obstacles, and the radii of repulsion, orientation, and attraction. ANOVAs showed significant interactions between the communication models and the number of agents ($F(2, 5398) = 11.26, p < 0.001$), the number of obstacles ($F(2, 5398) = 8.85, p < 0.001$), and the radius of attraction ($F(2, 5398) = 2.52, p = 0.043$). No significant interactions were found for the radii of orientation and repulsion.

Table 1 The search for a goal task descriptive statistics by models. The best means are in bold. (The percent reached, latency, and swarm clustering coefficient are represented by R , L , and SCC , respectively)

Model	Statistic	R	L	SCC
Metric	Mean	27.68	637.79	0.95
	Median	0.00	1000.00	0.95
	Std. Dev.	41.60	471.73	0.03
Topological	Mean	39.08	864.99	0.62
	Median	34.00	1000.00	0.62
	Std. Dev.	31.75	290.20	0.06
Visual	Mean	41.10	438.73	0.31
	Median	22.00	31.00	0.33
	Std. Dev.	42.56	487.99	0.07

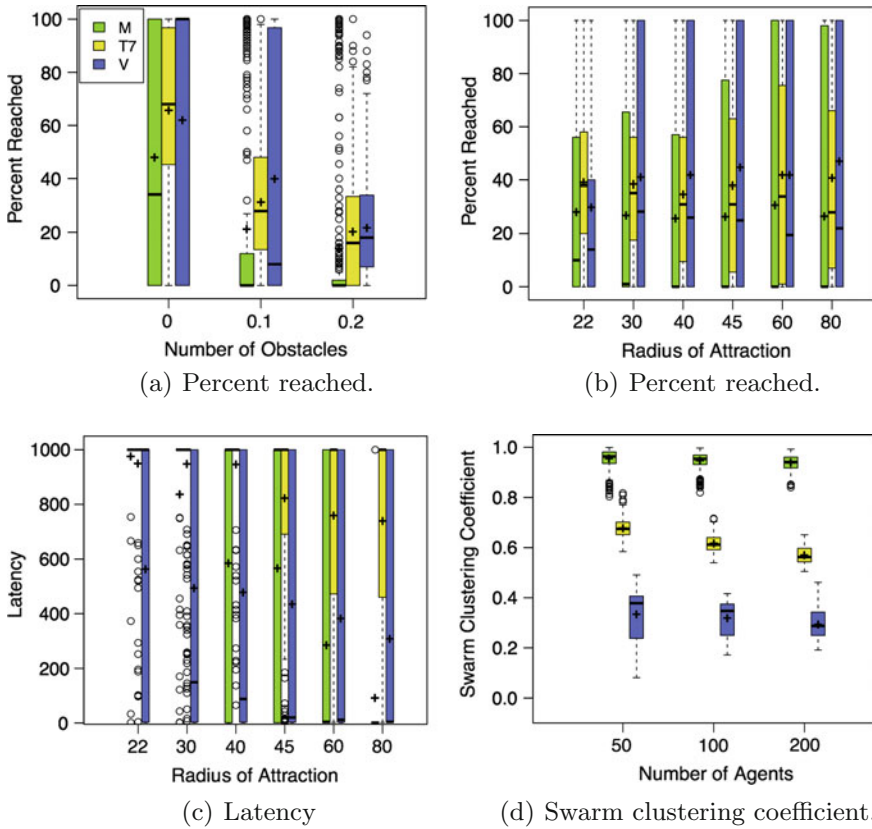


Fig. 4 The search for a goal task performance metrics. Each box plot denotes the first and third quartile of data. The *horizontal lines* indicate the medians, the crosses represent the means, and the *circles* show the outlying data. The legend for the plots **b–d** can be found in **a**, where *M*, *T7*, and *V* denote the metric, topological (with $n_{top} = 7$), and visual models, respectively

Fisher’s LSD test showed that for $N = 50$, there was no significant difference between the visual and topological models. The mean percent reached was the highest when $N = 100$ using the topological model. The visual model had the highest mean percent reached for $N = 200$. The percent reached for the metric model was significantly different compared to the other models across all values of N .

The mean percent reached for all the models decreased as additional obstacles were included, as shown in Fig. 4a.

At $r_{att} = 22.50$ there was no significant difference in percent reached for the metric and visual models, see Fig. 4b. The metric model’s mean percent reached was significantly higher at $r_{att} = 22.50$ compared to $r_{att} = 80$.

The means are susceptible to the influence of outliers, thus the median values are also reported as a central tendency measure to better assess the performance of the

communication models. Further, the interquartile ranges provide additional insights beyond the means.

The median for the metric model's percent reached was 0 for the overall results (see Table 1), which was much lower than the mean. The metric model's median was 0 for most of the parameters and their associated values. The exception being the largest value of N , the obstacle-free trials, the smallest values for the radii of repulsion and orientation, and the two smallest values for the radius of attraction. The median was typically below 10 for those cases, and less than 40 for the obstacle-free trials.

The visual model's third quartiles were at least 95 and mostly 100, except for when $N = 100$, $N_{obs} = 0.2$, and for the smallest values of the radii of orientation and attraction. The high third quartiles indicates that the fourth quartile, or the top 25% of the visual model trials, and at least one of the third quartile trials, had *all* agents reaching the goal area. The metric model's interquartile ranges had much larger variability than the topological model. Across the various parameters, there was at least one parameter value for which the metric model's third quartile was 100%.

Overall, the visual model's mean **latency** was the lowest, whereas the topological model had the highest mean latency, as presented in Table 1. ANOVA showed that a significant difference existed by communication model ($F(2, 5398) = 449.26$, $p < 0.001$). Moreover, pair-wise testing with Fisher's LSD test found that latency for all three models were significantly different from each other.

ANOVA found significant interactions by model and the number of agents ($F(2, 5398) = 45.70$, $p < 0.001$), number of obstacles ($F(2, 5398) = 40.60$, $p < 0.001$), radii of repulsion ($F(2, 5398) = 66.96$, $p < 0.001$), orientation ($F(2, 5398) = 28.59$, $p < 0.001$), and attraction ($F(2, 5398) = 11.15$, $p < 0.001$).

Fisher's LSD test showed that the visual model latency at $r_{att} = 22.50$ was significantly lower than the metric and topological models. At $r_{att} = 80$, the analysis found a significant difference across each of the models, with the metric model's mean latency being lowest (see Fig. 4c). An identical trend occurs for the lowest and highest radius of orientation.

The metric model's median latency was 1000, for most cases across the number of agents, number of obstacles, and the radii of repulsion, orientation, and attraction. The exceptions occurred for the largest value of the radius of repulsion, the two largest values of the radius of orientation, and the two largest values of the radius of attraction, as shown in Fig. 4c. The median latency was typically 0 for those exceptional cases. Similarly, the topological model's median latency was 1000 across the variables. Additionally, the first quartile of the topological model's latency was 1000 in most cases, and in certain cases, it was at least greater than 400 (see Fig. 4c). The visual models' median latency was lower than the mean, and was 0 for the largest value of the number of agents, the largest value of the radius of repulsion, and the two largest values of the radii of orientation and attraction (see Fig. 4c).

The mean **swarm clustering coefficient** was lowest in the visual model and highest in the metric model. An ANOVA showed a significant difference by model

($F(2, 5398) = 1810, p < 0.001$). Fisher's LSD test found that all the models had significantly different means.

Results from ANOVA showed that for the swarm clustering coefficient, there were significant interactions by model and the number of agents ($F(2, 5398) = 631.50, p < 0.001$), the number of obstacles ($F(2, 5398) = 2132.00, p < 0.001$), the radii of repulsion ($F(2, 5398) = 320.90, p < 0.001$), orientation ($F(2, 5398) = 144.40, p = 0.03$), and attraction ($F(2, 5398) = 166.40, p < 0.001$). The results of Fisher's LSD test found a significant pair-wise difference between the models across all variables and associated values.

The median swarm clustering coefficients for all communication models were generally close to the means across all parameters and associated values. The interquartile ranges were typically tight, with only a few cases where the maximum value of one model overlapped with the minimum value of another. Those cases were the smallest number of agents (see Fig. 4d), the smallest radii of repulsion, orientation, and attraction.

4.3 Discussion

H_{sg1} was partially supported. The topological and visual models outperformed the metric model in reaching the goal area, yet there was no clear difference between the visual and topological models.

The visual model latency was substantially lower than the topological and metric models; however, the metric model outperformed the topological model in terms of the transfer of information. As such, H_{sg2} was also only partially supported. The metric model's bidirectional communication links possibly allowed information to spread faster through the network, compared to the topological model.

Similar to Strandburg-Peshkin et al.'s [31] results for fish, the swarm clustering coefficient was lowest with the visual model. The clustering coefficient for fish with the topological model was higher than the metric model, contrary to the findings presented in Table 1. One possible reason for this difference can be attributed to the difference in using collective motion experimental data as opposed to modeling through self-propelled particles.

Based on the general findings, the visual communication model is the best for artificial swarms completing a search for a goal task when fewer redundant connections are desired, because it resulted in virtually the best percent reached, the lowest latency, and the lowest swarm clustering coefficient. A low swarm clustering coefficient can be disadvantageous in noisy environments, which can benefit from redundant communication links. The metric and topological models are preferred for such environments, because of their high swarm clustering coefficients. Furthermore, given a noisy environment and a requirement for only a few agents to reach the goal, then the metric model is preferred. Given the same noisy environment, but a high percentage of agents needed to reach the goal, then the topological model can be used. The tradeoff is the model's high latency.

The analysis by the radius of attraction, which was the value of d_{met} , revealed that the metric and visual models are fundamentally different from one another and the difference does not stem from the visual model’s larger communication range. Overall, the visual-based swarms performed better than the metric-based swarms. However, at the lowest value of the radius of attraction ($d_{met} = 22.50$), the metric and visual models had comparable mean percent reached. Furthermore, for the highest value of the radius of attraction, or $d_{met} = 80$, the latency of the metric model was shown to be significantly lower than the visual, which used a range of $d_{vis} = 425$.

5 The Avoid an Adversary Experiment

5.1 Experimental Design

This experiment was performed using the same machine and the experimental parameters, other than N_{obs} , were identical. No obstacles were included in this experiment.

The swarm is required to avoid a predator-like agent² during the *avoid an adversary* task, which is modeled through a repulsive force exerted by the adversary on the swarm agents [3]. The swarm (dark mass in Fig. 5a) is initially aligned facing the predator (triangle in Fig. 5a). The predator is the same size as the swarm agents and can occlude the visual communication between agents. For illustrative purposes, the rendering of the predator has been increased. The predator (moving in a predefined path) and swarm travel toward each other and when the swarm agents are within r_{att} of the adversary, the predator’s repulsive forces affect the swarm agents’ heading. Agent positions are initially distributed in an area that is proportional to the swarm’s size, N . The predator’s starting position is horizontally offset, such that the predator and swarm travel the same distance to meet, regardless of the swarm’s size. The effects of the adversary on the swarm are isolated by removing the environmental obstacles and negating the wall’s repulsive forces. Each trial runs for 200 iterations.

Dispersion, denoted by D , is measured as the percentage increase of the average agent to agent distance from the start to the end of the trial. The average agent to agent distance has significance in the biological literature and is one of eleven parameters considered when characterizing the emergent properties of fish [26].

A connected component is defined as the largest collection of agents in which any two agents are either connected directly by a communication link or indirectly via neighbors [13]. The *number of connected components*, CCO , is calculated at the end of a trial, and is 1 at the start of a trial.

The *percent isolated components*, represented by I , is the percentage of swarm agents that have no neighbors.

²Videos of example trials can be found at <http://eecs.vanderbilt.edu/research/hmtl/wp/index.php/research-projects/human-swarm-interaction/emulating-swarm-communications/>.

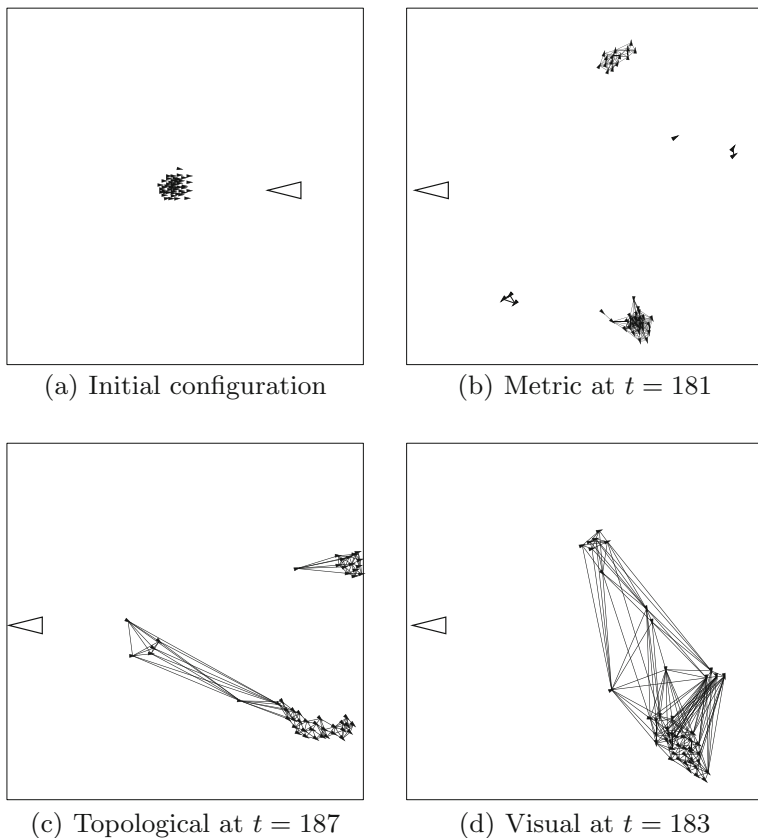


Fig. 5 An artificial swarm performing the avoid an adversary task under all three communication models. The adversary is denoted by a *triangle* and swarm's agents are represented by *filled triangles*. The lines between agents denote communication links. The trial parameters were: **b-d** $N = 50$, $r_{rep} = 10$, $r_{ori} = 15$, $r_{att} = 30$; **b** $d_{met} = 30$; **c** $n_{top} = 6$; **d** $d_{vis} = 425$

The three hypotheses for this task are:

1. $H_{aa1}: D_V < D_T < D_M$.
2. $H_{aa2}: CCO_V < CCO_T < CCO_M$.
3. $H_{aa3}: I_T < I_V < I_M$.

The subscripts indicate the communication models.

Hypothesis H_{aa1} assumes that the metric model will generate swarms with the highest dispersion due to fragmentation. Additionally, the topological and visual models are expected to attract outlying agents back into the main swarm after the adversary's attack, reducing the swarm's dispersion.

Hypothesis H_{aa2} states that swarms using the visual model will fragment into fewer connected components compared to the topological swarms, which will

fragment less than the metric-based swarms. The hypothesis is based on the metric model's limited sensing range.

By definition, the topological model does not produce any isolated agents for any $n_{top} \geq 1$. H_{aa3} in relation to the visual and metric models follows the same reasoning underlying H_{aa2} : the metric model's limited sensing range will lead to a higher percentage of isolated agents than the visual model.

The avoid an adversary task experiments were specified similarly to the search for a goal task. The total number of trials for the avoid adversary task was 3,600: 600 trials for the metric and the visual models, and 2,400 trials for the topological model (600 trials for each of the four values of n_{top}).

5.2 Results

Dispersion ($A = 70.16$, $p < 0.001$), number of connected components ($A = 179.90$, $p < 0.001$), and percent isolated components ($A = 296.44$, $p < 0.001$) were distributed normally according to the Anderson-Darling test. Similar to the prior experiment, n_{top} was set to 7, as the ANOVA found no significant interactions across the metrics by the topological number. Unlike the previous experiment, a detail account of the medians and quartile ranges are not reported as the medians were generally quite close to the means. Furthermore, the interquartile ranges were tight (see Fig. 6).

Overall, **dispersion** was the highest with the topological model and the lowest with the visual model (see Table 2). An ANOVA showed that model type had a significant impact on dispersion ($F(2, 5398) = 562.49$, $p < 0.001$). Fisher's LSD test found the mean dispersions to be significantly different across the three models.

ANOVAs revealed that the communication models had significant interactions for the number of agents ($F(2, 5398) = 118.32$, $p < 0.001$), the radius of repulsion ($F(2, 5398) = 363.27$, $p < 0.001$), the radius of orientation ($F(2, 5398) = 26.15$, $p < 0.001$), and the radius of attraction ($F(2, 5398) = 9.98$, $p < 0.001$).

Dispersion using the topological model was significantly higher compared to the metric and the visual models for all values of N . Fisher's LSD tests showed that the visual model dispersion was significantly lower compared to the metric model at $N = 50$. However, no significant difference between the metric and visual model dispersions was found for the other values of N (see Fig. 6a).

Fisher's LSD test found that the mean dispersion for the visual model was significantly lower than the metric model at $r_{rep} = 10$, but significantly higher than the metric model at $r_{rep} = 20$, as shown in Fig. 6b. Similarly, as the values of the radii of orientation and attraction increased, the metric model's dispersion decreased to a value significantly lower than the visual model.

ANOVA determined that model type had a significant impact on the **number of connected components** ($F(2, 5398) = 1776.23$, $p < 0.001$). This metric was significantly different between each of the communication models, as indicated by the Fisher's LSD test. The visual model had the lowest number of connected components, while metric had the highest, as shown in Table 2.

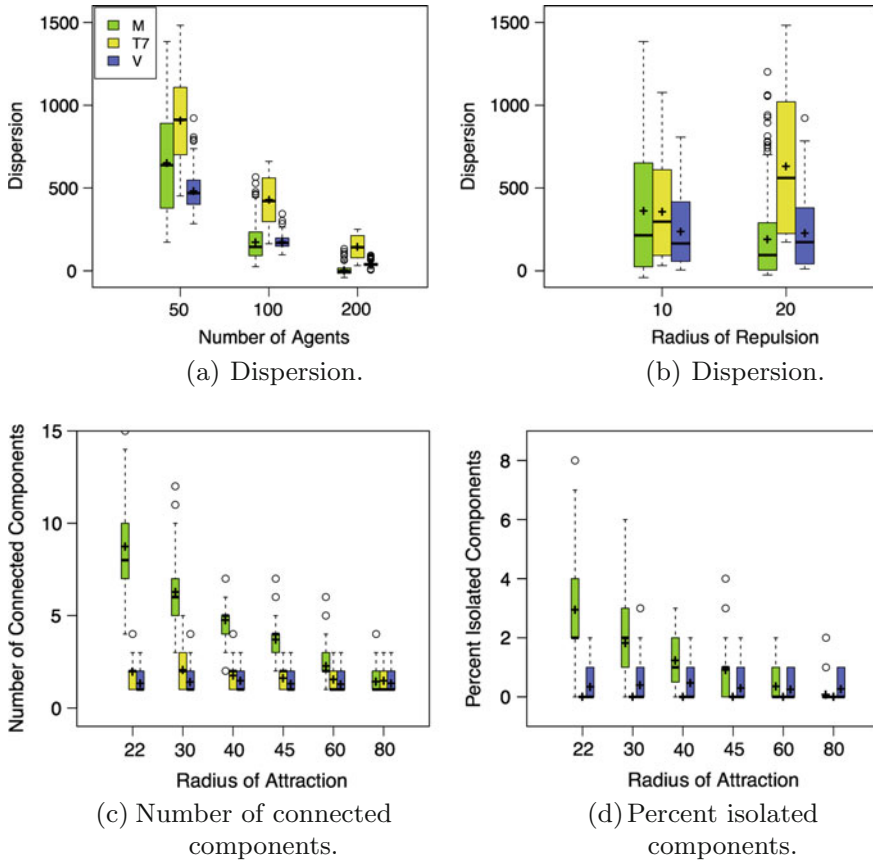


Fig. 6 The avoid an adversary task performance metrics. The legend for the plots **b–d** can be found in **a**, where *M*, *T7*, and *V* denote the metric, topological (with $n_{top} = 7$), and visual models, respectively

The ANOVAs found significant interactions by the number of agents ($F(2, 5398) = 5.25, p < 0.01$), and the radii of repulsion ($F(2, 5398) = 772.53, p < 0.001$), orientation ($F(2, 5398) = 133.89, p < 0.001$), and attraction ($F(2, 5398) = 53.72, p < 0.001$).

Fisher’s LSD test showed that the number of connected components was significantly different between all three models across the number of agents. Visual had the lowest number of connected components, whereas metric had the highest, for all values of N .

The metric model generated fewer connected components as the radius of attraction increased (see Fig. 6c). At $r_{att} = 80$, there was no significant difference between the metric and visual models in the number of connected components.

Table 2 The avoid an adversary task descriptive statistics by models. Dispersion, the number of connected components, and the percent isolated components are denoted by D , CCO , and I , respectively

Model	Statistic	D	CCO	I
Metric	Mean	275.61	4.46	1.19
	Median	144.71	4.00	1.00
	Std. Dev.	334.85	2.78	1.38
Topological	Mean	493.92	1.75	0.00
	Median	421.50	2.00	0.00
	Std. Dev.	356.32	0.79	0.00
Visual	Mean	232.03	1.35	0.33
	Median	168.68	1.00	0.00
	Std. Dev.	196.64	0.58	0.54

The visual model produced values for the **percent isolated components** that were typically lower than the metric model (Table 2). ANOVA found a significant difference across the communication models ($F(2, 5398) = 489.78, p < 0.001$), and Fisher's LSD test found that the models had significantly different means from each other.

ANOVAs indicated that communication models had significant interactions with the number of agents ($F(2, 5398) = 8.14, p < 0.001$), the radius of repulsion ($F(2, 5398) = 232.23, p < 0.001$), the radius of orientation ($F(2, 5398) = 32.24, p < 0.001$), and the radius of attraction ($F(2, 5398) = 29.28, p < 0.001$).

Similar to the connected components evaluations, the metric model's percent isolated components decreased as the size of the radii of repulsion, orientation, and attraction (see Fig. 6d) increased. At, $r_{att} = 80$, the metric model's percent isolated components was significantly lower than the visual model.

5.3 Discussion

The topological model produced the highest dispersion compared to the other models. H_{aa1} was only partially supported due to the topological's higher dispersion compared to the metric model.

H_{aa2} was fully supported, as the visual model produced the smallest number of connected components, whereas the metric model generated the highest number of connected components. The visual model's percent isolated components was lower than the metric model, which fully supports H_{aa3} .

A high dispersion in some biological species may serve to confuse a predator from singling out a particular swarm agent [3]. Thus, if a higher dispersion is preferred, the general findings indicate that the topological communication model is the best for the avoid an adversary task, because it offers the highest dispersion, paired with

low connected components, and no isolated components. A high dispersion can be disadvantageous if environmental features physically constrain the swarm's movement. The metric and the visual models are preferred for such environments, as they provide a lower dispersion. However, if a task requires a low percentage of isolated components, then the visual model is preferred, otherwise, the metric communication model will suffice.

The results across independent variables did not find the visual model's relatively larger communication range to provide an unfair advantage over the metric model. At the highest radius of attraction, or $d_{met} = 80$, there was no significant difference in number of connected components between the metric and visual models, despite d_{vis} being 425.

6 Practical Applications

This research is intended to serve as the foundation of a more complete examination of what factors impact swarm performance. To date, this research has focused on the set of behavior, environment, task, and hardware (BETH) as factors likely to impact swarm performance. The behavioral components in this research were the communication model used and the values set for the radii of repulsion, orientation, and attraction. The environmental variables in this research were the number of obstacles and the number of adversaries, but future research will explore other variables such as size of the area of deployment, environmental hazards, and characteristics of adversaries. This research only considered two tasks, search for a goal and avoid adversary, but these simple tasks form the basis of many more complex tasks with both military and civilian applications [7, 10]. The number of agents deployed to a task was the primary hardware limitation in this research, but as discussed in the previous section, the radii of repulsion, orientation, and attraction can be limited by hardware capabilities; other physical factors such as agent size and speed are outside the scope of this research, but future research needs to explore the impact these factors have singularly and in concert with the other components of BETH. Identifying the BETH variables that impact swarm performance and quantifying the effects of their interactions enables the development of a decision support software to optimize the likelihood of successful task completion for any given combination of known and unknown values of the components of BETH.

The body of research that explores decision support software (DSS) extends as far back as the 1970s and encompasses many different algorithms for processing the available information [25]. The goal of such software for operators of remotely deployed mobile robots is to provide decision support by simplifying the information presented to the operator [33]. A full examination of DSS and the design of interfaces for robot operators would far exceed the available space, and the design, implementation, and validation of such an interface requires its own lengthy research process. A simplified example of design and use of such an interface is given below

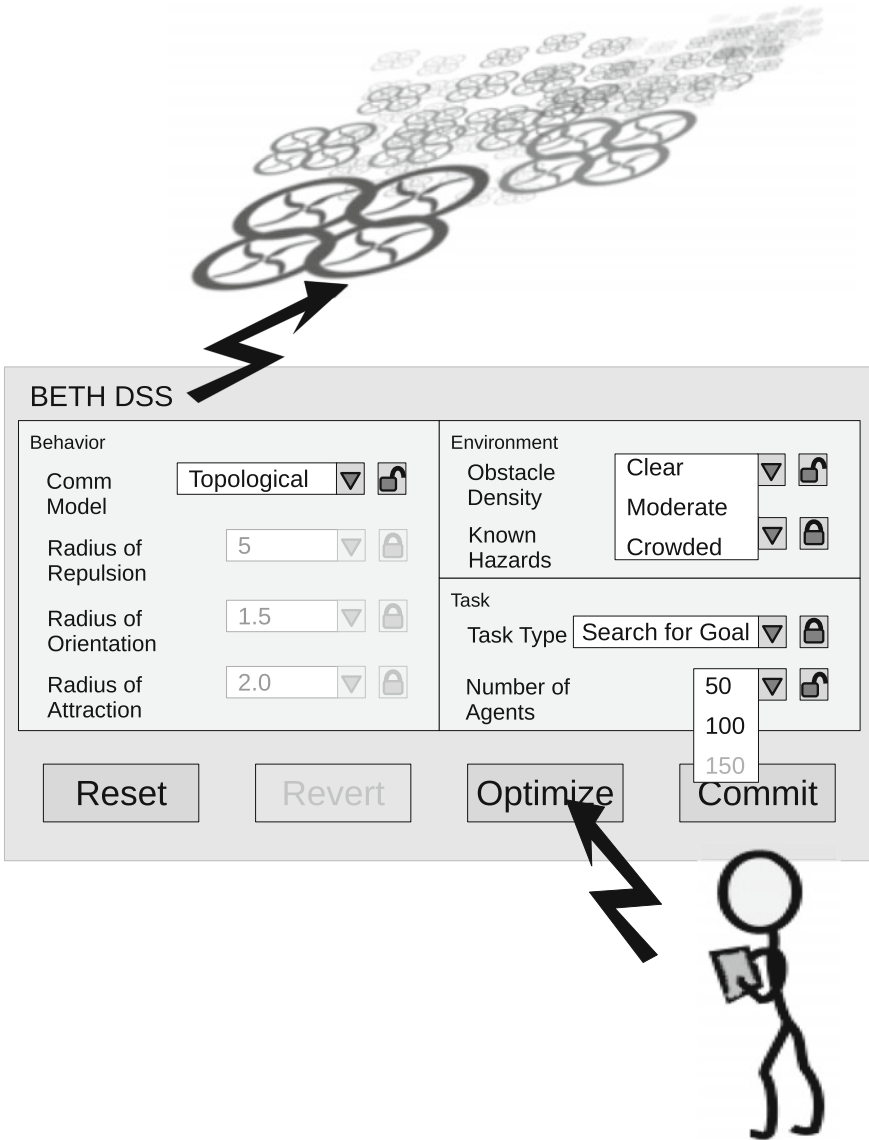


Fig. 7 An example interface using the BETH DSS model is shown. This simple wireframe illustrates how gathered data can reduce the decisions an operator needs to make in order to optimize the performance of a remotely deployed artificial swarm

to illustrate how knowledge of the factors that impact swarm performance can be used to support the operator of a robotic swarm.

Figure 7 shows an example interface that uses the BETH model to organize and simplify information for the operator deploying a swarm of robots. The available

performance factors are presented grouped by Behavior, Environment, and Task. Hardware factors that impact swarm performance are made implicit by limiting the behavior, environment, and task factors to values permitted by the available hardware, freeing the operator from tracking hardware capabilities.

To use the interface, the operator must select a Task Type. The operator can then assign values for as many of the remaining performance factors as desired. For example, the operator in Fig. 7 is creating a Search for a Goal task. The operator has specified the topological communication model, but has left the padlock button toggled to “unlocked.” Thus, the system is allowed to change the communication model during the optimization process, if a different model has a higher likelihood of success. The three radii of repulsion, orientation, and attraction are shown greyed out; the interface makes the information available but clearly indicates that the values of the radii cannot be changed by the operator (presumably the values are limited by the hardware capabilities of the swarm).

The operator has the option to supply information about the Environment where the swarm will be deployed; in this example the operator has provided a value for Known Hazards and is selecting a value for Obstacle Density. The operator has locked the Known Hazards field and left the Obstacle Density field unlocked, indicating that the system can adjust the Obstacle Density value if provided with new information, but that the information the operator has provided about the Known Hazards is to be assumed true even if the system cannot detect those hazards.

The Number of Agents can be set by the operator. The operator in the example the operator can choose between 50 and 100 agents although the value 200 is greyed out, indicating that some of the operators robots are otherwise engaged, lost, or damaged. The operator can press the Optimize button, and the system will validate the deployment variables. If the system determines that changing the values of any of the unlocked Behavior or Task variables will improve the likelihood of success, or if the system has updated information for any unlocked environmental variables, the system will update the variables with the new values, highlighting the fields that have changed so the operator understands the changes. When the operator is satisfied with the deployment configuration, pressing the “Commit” button sends the command to the swarm.

7 Discussion and Conclusion

The presented research focuses on a general hypothesis that the selection of communication model impacts the swarm’s task performance. The general findings demonstrated that there was a significant impact of model type on task performance. Further, the results show that the visual model resulted in the best overall task performance for the search for a goal task, while the best overall performance was achieved with the topological model for the avoid an adversary task. The relevance of this outcome is that the intelligence of a remotely deployed swarm is amplified through the deliberate selection of a communication model. Additional analysis of typical arti-

ficial swarm tasks is necessary to fully support the general hypothesis; however, the presented results provide preliminary evidence that artificial swarm design needs to consider the communication model and task pairing in order to optimize the overall swarm performance.

Based on the presented search for a goal and avoid an adversary task results, connections can be made to the biological swarm literature. Couzin et al. [12] showed that the size of the radius of repulsion did not have an effect on the transitions between different swarm movement patterns. Rather, the relative sizes of the radius of orientation to the radius of repulsion and the radius of attraction to the radius of orientation produces the transitions. For instance, simulated swarms rotate in a torus when the ratio of the radius of orientation to the radius of repulsion is relatively low and the ratio of the radius of attraction to the radius of orientation is relatively high. Presented results for the search for a goal task conform to Couzin et al.'s [12] results in relation to the radius of repulsion. The duration of this task (1000 iterations) resulted in trials that demonstrated swarm movement patterns, as found by Couzin et al. Similar results were expected for the avoid an adversary task; however, were not found due to the task's short duration (200 iterations).

The scope of the reported research does not follow the so-called prescriptive agenda where the values of the model parameters are free design choices [22, 30]; thus, d_{vis} is not varied. This line of inquiry will become necessary when prescribing the communication models to specific platforms, such as the s-bots, which are equipped with proximity and vision sensors [24]. Analyzing the effects of varying model parameters, such as d_{met} and d_{vis} will also be necessary due to differences in the communication ranges across the platforms that will attempt to adopt the models. For instance, the metric model can be realized with omni-directional antennas, as well as infrared LED sensors. The LED range is considerably smaller (10 cm in Kilobots [28]). Similarly, exploring the effects of different values of n_{top} will be useful. The topological model can be implemented using band-limited communication channels [16], and for infrared-based, band-limited platforms, such as the r-one, n_{top} will be inversely related to the maximum communication range [23].

Acknowledgements This material is based upon research supported by, or in part by, the U.S. Office of Naval Research under award #N000141210987.

References

1. Abaid, N., Porfiri, M.: Fish in a ring: spatio-temporal pattern formation in one-dimensional animal groups. *J. R. Soc. Interface* 7(51), 1441–1453 (2010)
2. Aoki, I.: A simulation study on the schooling mechanism in fish. *Bull. Japan. Soc. Sci. Fish.* 48(8), 1081–1088 (1982)
3. Ballerini, M., Cabibbo, N., Candelier, R., Cavagna, A., Cisbani, E., Giardina, I., Lecomte, V., Orlandi, A., Parisi, G., Procaccini, A., Viale, M., Zdravkovic, V.: Interaction ruling animal collective behavior depends on topological rather than metric distance: evidence from a field study. *PNAS* 105(4), 1232–1237 (2008)

4. Barberis, L., Albano, E.V.: Evidence of a robust universality class in the critical behavior of self-propelled agents: metric versus topological interactions. *Phys. Rev. E* **89**(1), 9–26 (2014)
5. Bode, N.W.F., Frank, D.W., Wood, A.J.: Limited interactions in flocks: relating model simulations to empirical data. *J. R. Soc. Interface* **8**, 301–304 (2011)
6. Bonabeau, E., Dorigo, M., Theraulaz, G.: *Swarm intelligence: from natural to artificial systems*. Oxford University Press, New York, NY (1999)
7. Bonabeau, E., Dorigo, M., Theraulaz, G.: *Swarm Intelligence: From Natural to Artificial Systems*, No. 1. Oxford University Press (1999)
8. Camazine, S., Deneubourg, J.L., Franks, N.R., Sneyd, J., Theraulaz, G., Bonabeau, E.: *Self-Organization in Biological Systems*. Princeton University Press, Princeton, NJ (2003)
9. Cianci, C.M., Raemy, X., Pugh, J., Martinoli, A.: Communication in a swarm of miniature robots: the e-puck as an educational tool for swarm robotics. In: *Proceedings of the 2nd International Conference on Swarm Robotics*, pp. 103–115 (2007)
10. Clough, B.T.: Uav swarming? so what are those swarms, what are the implications, and how do we handle them?. Technical report, DTIC Document (2002)
11. Couzin, I.D., Krause, J., Franks, N.R., Levin, S.A.: Effective leadership and decision-making in animal groups on the move. *Nature* **433**, 513–516 (2005)
12. Couzin, I.D., Krause, J., James, R., Ruxton, G.D., Franks, N.R.: Collective memory and spatial sorting in animal groups. *J. Theor. Biol.* **218**(1), 1–11 (2002)
13. Easley, D., Kleinberg, J.: *Networks, Crowds, and Markets: Reasoning About a Highly Connected World*. Cambridge University Press, New York, NY (2010)
14. Ferrante, E., Turgut, A.E., Mathews, N., Birattari, M., Dorigo, M.: Flocking in stationary and non-stationary environments: a novel communication strategy for heading alignment. In: *Parallel Problem Solving from Nature*, pp. 331–340 (2010)
15. Goodrich, M., Kerman, S., Pendleton, B., Sujit, P.: What types of interactions do bio-inspired robot swarms and flocks afford a human? In: *Proceedings of Robotics: Science and Systems*, pp. 105–112 (2012)
16. Goodrich, M.A., Sujit, P., Kerman, S., Pendleton, B., Pinto, J.: Enabling human interaction with bio-inspired robot teams: topologies, leaders, predators, and stakeholders. Technical Report BYU-HCMI 2011-1, Computer Science Department, Brigham Young University, Provo, USA, Aug 2011
17. Huth, A., Wissel, C.: The simulation of the movement of fish schools. *J. Theor. Biol.* **156**, 365–385 (1992)
18. Kolling, A., Walker, P., Chakraborty, N., Sycara, K., Lewis, M.: Human interaction with robot swarms: a survey. *IEEE Trans. Hum.-Mach. Syst.* **46**(1), 9–26 (2016)
19. Kolpas, A., Busch, M., Li, H., Couzin, I.D., Petzold, L., Moehlis, J.: How the spatial position of individuals affects their influence on swarms: a numerical comparison of two popular swarm dynamics models. *PLoS ONE* **8**(3), e58525 (2013)
20. Krause, J., Ruxton, G.D.: *Living in Groups*. Oxford University Press, New York, NY (2002)
21. Maçãs, C., Cruz, P., Martins, P., Machado, P.: Swarm systems in the visualization of consumption patterns. In: *Proceedings of the Twenty-Fourth International Joint Conference on Artificial Intelligence*, pp. 2466–2472 (2015)
22. Mannor, S., Shamma, J.: Multi-agent learning for engineers. *Artif. Intell.* **171**(7), 417–422 (2007)
23. McLurkin, J., McMullen, A., Robbins, N., Habibi, G., Becker, A., Chou, A., Li, H., John, M., Okeke, N., Rykowski, J., Kim, S., Xie, W., Vaughn, T., Zhou, Y., Shen, J., Chen, N., Kaseman, Q., Langford, L., Hunt, J., Boone, A., Koch, K.: A robot system design for low-cost multi-robot manipulation. In: *Proceedings of the IEEE/RSJ International Conference on Intelligent Robots and Systems (IROS)* (2014)
24. Mondada, F., Gambardella, L.M., Floreano, D., Nolfi, S., Deneubourg, J.L., Dorigo, M.: The cooperation of swarm-bots: physical interactions in collective robotics. *Robot. Autom. Mag.* **12**(2), 21–28 (2005)
25. Nunamaker, J.F., Applegate, L.M., Konsynski, B.R.: Computer-aided deliberation: model management and group decision support: special focus article. *Oper. Res.* **36**(6), 826–848 (1988)

26. Parrish, J.K., Viscido, S.V., Grünbaum, D.: Self-organized fish schools: an examination of emergent properties. *Biol. Bull.* **202**, 296–305 (2002)
27. Reynolds, C.: Flocks, herds and schools: a distributed behavioral model. *Comput. Graph.* **21**(4), 25–34 (1987)
28. Rubenstein, M., Ahler, C., Nagpal, R.: Kilobot: A low cost scalable robot system for collective behaviors. In: *Proceedings of the IEEE International Conference on Robotics and Automation (ICRA)* (2012)
29. Shang, Y., Bouffanais, R.: Consensus reaching in swarms ruled by a hybrid metric-topological distance. *Eur. Phys. J. B* **87**(294) (2014)
30. Shoham, Y., Powers, R., Grenager, T.: If multi-agent learning is the answer, what is the question? *Artif. Intell.* **171**(7), 365–377 (2007)
31. Strandburg-Peshkin, A., Twomey, C.R., Bode, N.W., Kao, A.B., Katz, Y., Ioannou, C.C., Rosenthal, S.B., Torney, C.J., Wu, H.S., Levin, S.A., Couzin, I.D.: Visual sensory networks and effective information transfer in animal groups. *Curr. Biol.* **23**(17), R709–R711 (2013)
32. Vicsek, T., Czirók, A., Ben-Jacob, E., Cohen, I., Shochet, O.: Novel type of phase transition in a system of self-driven particles. *Phys. Rev. Lett.* **75**(6), 1226–1229 (1995)
33. Yanco, H.A., Drury, J.: Classifying human-robot interaction: an updated taxonomy. In: *2004 IEEE International Conference on Systems, Man and Cybernetics*, vol. 3, pp. 2841–2846. IEEE (2004)



<http://www.springer.com/978-3-319-66789-8>

Advances in Hybridization of Intelligent Methods

Models, Systems and Applications

Hatzilygeroudis, I.; Palade, V. (Eds.)

2018, IX, 147 p. 44 illus., 23 illus. in color., Hardcover

ISBN: 978-3-319-66789-8